Knowledge Consortium of Gujarat
Department of Higher Education - Government of Gujarat
Journal of Science - ISSN : 2320-0006

Continuous Issue - 19 | February – March 2019

THEORETICAL STUDY OF Pd39Ni10Cu30P21 BULK METALLIC GLASS USING TG and BS APPROACHES

ABSTRACT

The study of a bulk metallic glass (BMG) is an effective tool to find its advanced and hi-tech applications in various fields. The $Pd_{39}Ni_{10}Cu_{30}P_{21}$ BMG is theoretically studied in terms of longitudinal and transverse mode of phonon eigen frequencies in terms of the vibrational dynamics using two computational approaches given by Takeno-Goda (TG) and Bhatia-Singh (BS) under three local field correction functions viz. Ichimaru–Utsumi (IU), Farid et al. (F) and Sarkar et al. (S). The electron-ion interactions are represented by a well-established model potential with widely accepted local field correction functions. Here, pair correlation function (PCF) $g(r)$ is generated theoretically from interatomic pair potential V(R). The computed results of the phonon dispersion curves (PDC) produce respective phononic nature in the BMG. The theoretically computed thermodynamic and elastic properties are found in good agreement with the other such and experimental data available in the literature.

KEY WORDS: *Bulk metallic glass, Interatomic pair potential, Pair correlation function, Phonon dispersion curve, Thermodynamic properties, Elastic properties.*

1. INTRODUCTION

1.1 Bulk Metallic Glasses:

For decades, metallic glasses have been a field of continual interest due to their uncommon properties and unique structure leading to exciting technological promises. Their properties like high fracture strength, soft magnetism, admirable wear and corrosion resistances, anomalous electronic transport properties etc. make BMGs an expected choice for the new engineering materials in several applications including prosthetic devices, sports materials, fashion jewelries, scientific instruments, data storage devices, device-case, outer body of space vehicle etc. A BMG is an amorphous alloy, which exhibits liquidus temperature below melting point of its constituent elements. It works as an atomically frozen liquid that form glassy solids with a unique amorphous atomic structure having high yield strength and high elastic limit under shock impact conditions that lacks slips planes. Why BMGs have been attracting strong interest? They serve to highlight some of the challenging issues awaiting for resolutions from the researchers.[**1**, 2].

1.2 Past study of $Pd_{39}Ni_{10}Cu_{30}P_{21}$ BMG:

The quaternary BMG $Pd_{39}Ni_{10}Cu_{30}P_{21}$ has substantial potentials for studying its extraordinary glass forming ability (GFA), wide super-cooled liquid regions, highest reduced glass transition temperature; and they can be prepared into glass with a maximum thickness of over 70 mm at a cooling rate less than 1 K/s [**3**, **4**]. It shows increased ductility even by the homogeneous dispersion of spherical pores into glassy matrix. In addition to increased ductility, its porous state exhibits a decline in Young's modulus, specific weight and strength but rise in absorption energy up to fracture. This BMG has dense random packed atomic configuration. Since the metallic elements in this BMGs are of FCC structure, it is likely that its atomic configuration is close to that of the crystalline FCC structure. $Pd_{39}Ni_{10}Cu_{30}P_{21}$ BMG, at room temperature up to 23.5 GPa, reveals pressure-induced structural relaxation. Progressively elevated pressure gives rise to structural stiffness of the BMG, which results in a smaller pressure dependence of the volumetric change [**5**]. While transition from glassy state to super cooled liquid and crystalline structure, it results in formation of coarse-grained spongy structures [**6**, **7**]. Its density, molar mass, glass transition temperature and fragility are 9.152 $g\backslash cm^3$, 72.9 $g/mole$, 586 K and 55 respectively as calculated by Jiang and Dai [**8**]. Levin *et al.* [**9**] studied the elastic properties of this BMG at different temperatures and densities using micro-acoustical technique.

1.3 Present Investigation:

In the present computational work, the pseudopotential theory [**1**, **2**] is applied to study some of the thermodynamic and elastic properties through vibrational dynamics of $Pd_{39}Ni_{10}Cu_{30}P_{21}$ BMG. Its phonon frequencies are obtained using two main computational approaches developed by Takeno-Goda (TG) [**11**, **12**] and Bhatia-Singh (BS) [**13**, **14**]. The screening influence on the properties of $Pd_{39}Ni_{10}Cu_{30}P_{21}$ BMG is studied by three local field correction functions viz. Ichimaru–Utsumi (IU) **[17]**, Farid *et al*. (F) **[18]** and Sarkar *et al.* (S)[**19**]. The thermodynamic properties viz. transverse sound velocity (υ_T), longitudinal sound velocity (υ_L), Debye temperature (θ_D); and also, some elastic properties such as Young's modulus (Y), modulus of rigidity (G), isothermal bulk modulus (B_T), Poisson's ratio (σ) are computed using PDC [**1**, **2**].

2. THEORETICAL METHODOLOGY

The application of pseudopotential to BMGs involve the assumption of 'pseudo-ions' with average properties that replace three types of ions in the BMGs, and the electron gas is supposed to infuse through them. The existence of electron–pseudo-ion is possible due to the pseudopotential and the electron-electron interaction involved through a dielectric screening function. The mathematical illumination on Shaw's constant core model potential [**20**] is,

$$W(q) = -\frac{8\pi Z}{\Omega_0 q^2}\left[\frac{\sin \boldsymbol{q} r_c}{\boldsymbol{q} r_c}\right]. \qquad (01)$$

here, **q** is the wave vectors, Z is valence and Ω_0 is atomic volume. The model potential parameter r_C is obtained by fitting either to some experimental data or to realistic form-factors or other data relevant to the properties investigated. The pseudopotential parameter is so fixed that it may generate a PCF accurately consistent with the experimental data found in the literature. The electron-ion interactions for BMGs can be explained meaningfully PAA model instead of Vegard's law [**1**, **2**].

The quaternary BMG system $A_pB_qC_r\,D_s$ (where p, q, r and s are the proportionate concentration of the concerned element) is considered to be a multi-component fluid of the bare mixed ions occupied in a uniform electron gas. If the pair potentials of the single components are known, the mean effective density dependent interatomic pair potential V(r) can be explained successfully [**21**]. Here, the fundamental component pair potential [**15**, **20**, **22**] is given by,

$$V(r) = V_s(r) + V_b(r) + V_r(r). \qquad (02)$$

The contribution from the s-electron to the pair potential $V_s(r)$ is then,

$$V_s(r) = \left[\frac{Z_s{}^2 e^2}{r}\right] + \left(\frac{\Omega_0}{\pi^2}\right)\int F(q)\left[\frac{\sin(qr)}{qr}\right] q^2\, dq \qquad (03)$$

Where, Ω_0 is the effective atomic volume of the mono-component fluid and r is the core radius.

Here, the number of s-valance electron $Z_s \cong 1.5$ is obtained by integrating the partial S-density of states, which result from the self-consistent band structure computation for the entire $3d$ series and $4d$ series, Z_d is the number of d-electrons contributing to the interatomic pair-potential [**1**, **2**, **23**].

$$V_b(r) = -Z_d\left(1-\frac{Z_d}{10}\right)\left(\frac{12}{N}\right)^{\frac{1}{2}}\left(\frac{28.6}{\pi}\right)\left(2\frac{r_d^3}{r^5}\right) \qquad (04)$$

$V_b(r)$ allows the Friedel-model band broadening contribution to the transition-metal cohesion.

$$V_r(r) = Z_d\left(\frac{450}{\pi^2}\right)\left(\frac{r_d^6}{r^8}\right). \qquad (05)$$

Here, $V_r(r)$ arises from the repulsion of the d-electron muffin-tin orbitals on different sites due to their non-orthogonality. Wills and Harrison [**23**] studied the effects of the s-band and d-band. Where, $f(q)$ is the local field correction function, Z is Valance and ħ is the Plank's constant. m_e and e are mass and charge of an electron respectively

For BMG, the model potential parameter r_c **[1, 2, 23]** is given below.

$$\boldsymbol{r_c} = \left[\frac{(0.51)\, r_S}{(Z)^{1/3}}\right] \qquad (06)$$

Where, r_s is the Wigner Seitz radius of the BMG.

The input parameters and constants used for computation are given in **table: 1**.

Table 1: Input parameters and Constants useful in the computational work.

Z	Z_S	Z_d	R_d (au)	R_s (au)	Ω_0 $(au)^3$	N_C	M (amu)	r_c (au)
2.92	1.50	7.02	1.63	2.0209	100.95	9.48	72.93	0.7211

The parameters $Z_s, Z_d,\ r_d$ and N are determined from the band structure data of the pure metallic component which are already found in the literature **[1, 2, 23]** and obtained by the following expressions related to PAA model in the pseudopotential theory.

$$Z_d = pZ_{dA} + qZ_{dB} + rZ_{dC} + sZ_{dD} \quad (07)$$

$$Z_s = pZ_{sA} + qZ_{sB} + rZ_{sC} + sZ_{SD} \quad (08)$$

$$r_d = pr_{dA} + qr_{dB} + rr_{dC} + sr_{dD} \quad (09)$$

$$\mathrm{N} = pN_A + qN_B + rN_C + sN_D \quad (10)$$

Z_A , Z_B , Z_c, Z_D and Z is valency with p, q, r and s are the respective concentrations of different elements of the BMG in the form of $A_pB_qC_rD_s$. The PCF $g(r)$ is as important as the pair potential V(r) in studying a BMG **[1, 2, 24]**.

$$g(r) = \exp\left[\left(\frac{-V(r)}{k_BT}\right) - 1\right]. \quad (11)$$

The mathematical notations and theoretical analysis are well discussed in the respective papers of TG- and BS- approaches [$\mathbf{10-13}, \mathbf{22}, \mathbf{25-27}$]. The mathematical expressions of the longitudinal sound velocity v_L and the transverse sound velocity v_T ,which are computed from the long-wavelength limits of the PDC **[1, 2, 10-14]**.

$$\therefore\ \omega_L = v_L\, q \quad \text{and} \quad \omega_T = v_T\, q. \quad (12)$$

Young's modulus Y, Isothermal bulk modulus B_T, Modulus of rigidity G, Poisson's ratio σ and the Debye temperature θ_D are also computed by the expressions **[1, 2]** given below.

$$B_T = \rho\left[{v_L}^2 - \frac{4}{3}\,{v_T}^2\right] \quad (13)$$

$$\mathrm{G} = \rho\,{v_T}^2 \quad (14)$$

$$\sigma = \frac{1-2\left({v_T}^2/{v_L}^2\right)}{2-2\left({v_T}^2/{v_L}^2\right)} \quad (15)$$

$$Y = 2G(\sigma + 1) \quad (16)$$

$$\theta_D = \frac{\hbar\omega_D}{k_B} = \frac{\hbar}{k_B}2\pi\left[\frac{9\rho}{4\pi}\right]^{1/3}\left[\frac{1}{{v_L}^3} + \frac{2}{{v_T}^3}\right]^{-1/3} \quad (17)$$

Here, ω_D is the Debye frequency, ρ is isotropic number density.

3. RESULTS AND DISCUSSION:

3.1 Interatomic Pair Potentials:

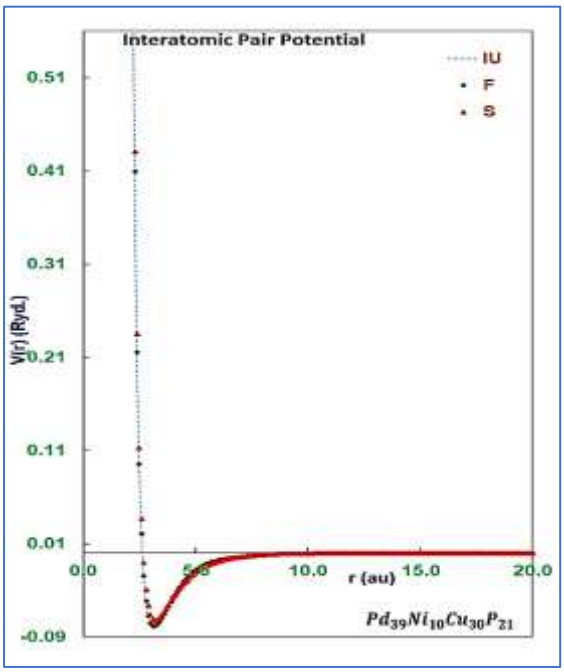

Figure 1: Inter atomic Pair Potentials of $Pd_{39}Ni_{10}Cu_{30}P_{21}$ BMG.

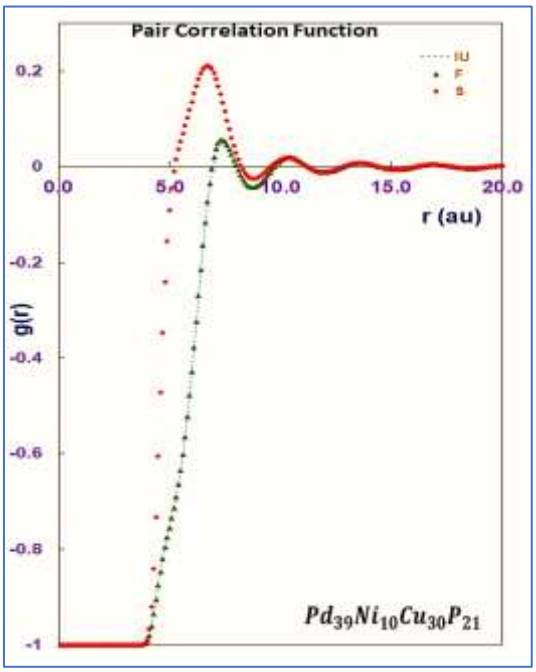

Figure 2: Pair Correlation Function of $Pd_{39}Ni_{10}Cu_{30}P_{21}$ BMG.

The screening dependency on the interatomic pair potentials plotted by Pair potential $V(r)$ (Ryd.) versus Interatomic distance r (au) in **Figure 1**. It reveals that the pattern of the interatomic pair potential V(r) is notably changed under exchange and correlation effects in the static H-dielectric screening. The 1st zero of the interatomic pair potentials $V\ (r = r_0)$, due to all local field correction functions, occurs at $r_0 = 2.7$ au**.** The nature of the screening affects interatomic pair potential V(r), well-width and its minimum position $V(r)_{min}$. The potential depth goes deep with increment of effective volume Ω_0. Various screening functions influence and slightly increase well-depth. In the pair potential, the depth is seen at $r = 3.2\ au$ for the selected screening functions. Present results do not show any oscillating behaviour. The potential energy is constantly remaining negative within the large $r-$ region. Thus, the part of this plot showing Coulomb repulsive potential dominates the oscillations due to electron-ion-electron interactions, which makes a negligibly minor waving shape after $r = 8.7\ au$. In the attractive part, interatomic pair potentials converge to a finite value instead of being zero. All interatomic pair potentials display the combined effect of $s-$and $d-$electrons. The repulsive part of the interatomic pair potential $V(r)$ is drawn lower and its attractive part is deeper due to the $d-$electron effect with when the $V(r)$ is shifted towards the lower r $-$values. Thus, the derived results seem to support $d-$0electron effect [**28**].

3.2 Pair Correlation Functions:

Figure 2 shows the PCF $g(r)$ prepared from the Interatomic pair potential, shows the screening effect. For the IU-, F- and S-functions respectively, the 3rd (atomic shell distance) peak (r_3) is found at 13.6, 13.6 and 13.5 au respectively, the 2nd (atomic shell distance) peak (r_2) is found at 10.4, 10.4 and 10.3 au respectively, while the nearest neighbouring distances (r_1)are found at 7.4, 7.4 and 6.8 au respectively. The ratio (r_2/r_1) is found 1.41, 1.41 and 1.54, while that of (r_3/r_1) is found 1.84, 1.8 and 2.01 for IU-, F- and S-function respectively. For these three local field correction functions, the mean ratio of 2nd to 1st peak is around 1.45, which is nearer to the characteristics for the disordered yet closed pack crystallographic structures and the mean ratio of the 3rd to 1st peak is nearly found 1.88 that suggests incomplete amorphisation of the samples **[28]**. These both ratios suggest that the atomic arrangement of the structure influences the short-range order of nearest neighbours. A large main peak at the nearest-nearest distance is followed by some smaller peaks corresponding to some more distant neighbours. One cannot make any specific remarks for the disorder after r~10.1 au

because the PCFs due to all functions mostly overlap each other from there. The long-range order is normal due to the waving shape of the interatomic pair potential V(r).

3.3 Phonon Dispersion Curves:

The PDC of $Pd_{39}Ni_{10}Cu_{30}P_{21}$ BMG was theoretically investigated by Chaudhari *et al*. [**29**] using a different bare ion model potential formalism by H- and T- local field corrections functions under HB- and BS- approaches. Wang [8, 9] has experimentally studied properties of this BMG using ultrasonic technique.

Figures **3** and **4** show the 'phonon eigen frequencies' for longitudinal and transverse phonon modes, computed with TG– and BS– approaches respectively with the three screening functions Viz. I-, F and S. The obtained vibrational properties based upon pseudopotential theory for this BMG agree with the other such [**29**, **30**] and experimentally generated [**9**, **31**, **32**] data already available in the literature. The inclusion of exchange and correlation effect increases the phonon eigen frequencies for both longitudinal and transverse modes.

The 1st minima for the longitudinal frequency ($\omega_{L\,min}$) in the TG-approach, it is found around $q \approx 2.8, 2.8$ and 3.5 Å^{-1} for IU- F- and S- functions respectively, while in the BS-approach, the same is found around $q \approx 1.6$ Å^{-1} for the selected functions. Typically, the dispersion relations express a minimum near $\boldsymbol{q}_p$, the wave-vector where the static structure factor $S(q)$ of the glass has its 1st maximum. The 1st maxima for the longitudinal frequency ($\omega_{L\,max}$) in the TG-approach, it is found around at $q \approx 1.4, 1.4$ and 1.8 Å^{-1} for IU-, F- and S-.

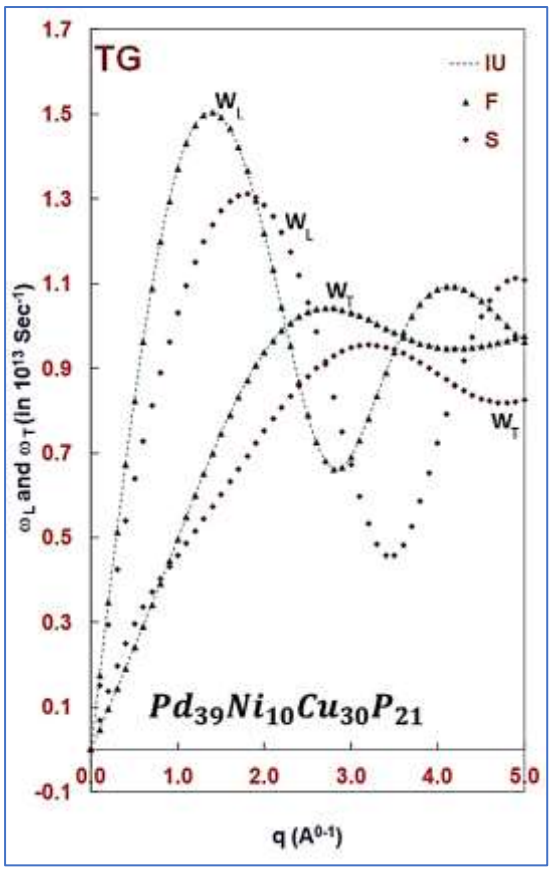

Figure 3: Phonon Dispersion Curves of $Pd_{39}Ni_{10}Cu_{30}P_{21}$ BMG (TG approach).

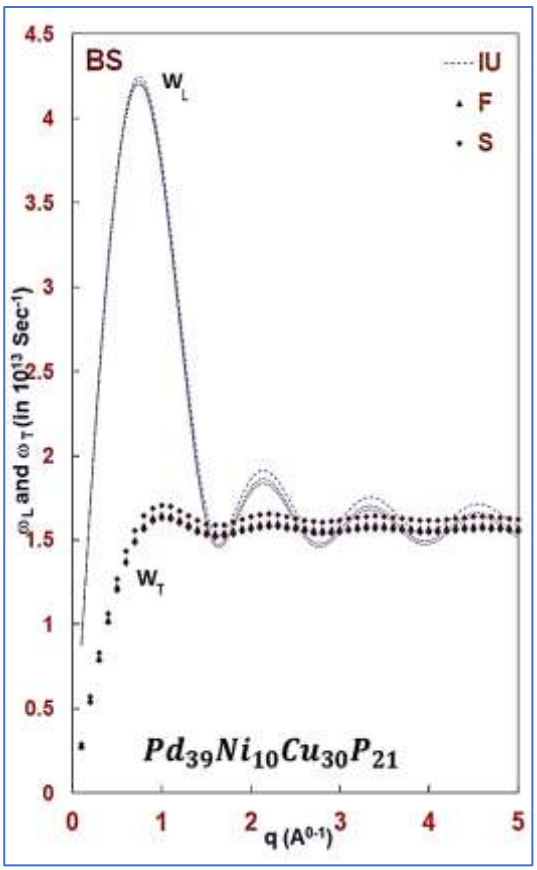

Figure 4: Phonon Dispersion Curves of $Pd_{39}Ni_{10}Cu_{30}P_{21}$ BMG (BS approach).

Functions while in BS-approach, the 1st maxima for the longitudinal frequency ($\omega_{L\,max}$) is found around $q \approx 0.6, 0.7$, and 0.7 Å^{-1} for IU- F- and S- local field correction functions respectively.

In the TG approach, the 1st minima in transverse frequencies ($\omega_{T\ min}$) is found at $q \approx 4.2,\ 4.1$ and 4.8 Å^{-1} respectively for the IU-, F- and S- functions. In the BS approach, the same is found at $q \approx 1.6\ \text{Å}^{-1}$ for all functions. For the transverse branch ($\omega_{T\ max}$), the 1st maxima in the TG approach, is found around at $q \approx 2.7, 2.7$ and $3.2\ \text{Å}^{-1}$ for IU-, F- and S- local field correction functions respectively. Similarly, in BS approach, the 1st maxima for the transverse branch ($\omega_{T\ max}$) is found at $\approx 1.0\ \text{Å}^{-1}$ for all functions.

The 1st crossover position of ω_L and ω_T in the TG-approaches is seen at $q \approx 2.3, 2.3$ and 2.7 Å^{-1} for IU- and F- and S- functions respectively. In the BS approach, nothing can be stated about such crossover position as it seems vague due to major overlapping on each other. In the transverse branch of BS approach, the frequencies increase with the wave vector q and then saturates at $\mathbf{q} \approx 1.0\ \text{Å}^{-1}$. This supports the Thorpe model **[33]** that a solid glass contains finite liquid clusters. The transverse phonons are absorbed for such frequencies as they are larger than the smallest eigen frequencies of the largest cluster.

The PDCs disclose that the longitudinal mode oscillations are more prominent than that of the transverse one. The instability of the transverse mode oscillations is result of anharmonicity of the atomic vibration in the BMG system. The collective excitations at larger momentum transfer is because of the prominence of longitudinal mode vibrations only.

3.4 Elastic and Thermodynamic Properties:

Table 2 : Elastic and Thermodynamic properties of $Pd_{39}Ni_{10}Cu_{30}P_{21}$ BMG.

Approach	Screening Function	$v_L \times 10^5\ cm/s$	$v_T \times 10^5\ cm/s$	$B_T \times 10^{11}\ \frac{dyne}{s^2}$	$G \times 10^{11}\ \frac{dyne}{s^2}$	σ	$Y \times 10^{11}\ \frac{dyne}{s^2}$	θ_D K
TG	IU	1.6117	0.4747	1.8591	0.1824	0.4525	0.5298	65.41
	F	1.6083	0.4733	1.8518	0.1813	0.4526	0.5267	65.22
	S	1.4625	0.7018	1.1245	0.3737	0.3504	1.0092	107.34
BS	IU	5.2938	1.682	19.6295	2.2898	0.4439	6.6122	231.53
	F	5.2772	1.6586	19.5711	2.2265	0.4452	6.4356	228.35
	S	5.323	1.7486	19.6336	2.4747	0.4395	7.1247	240.57
Others (Theoretical Data)	[**29**]	3.40 3.82 4.72	1.96 2.20 1.95	7.143 11.21 16.0	3.571 4.483 3.317	0.25 0.397	8.928 8.967 9.266	274.86 307.96 300.54
	[**29**]	---	---	15.91	3.51	---	---	---
	[**30**]	4.750	1.963	15.94 15.91 15.87 15.85	3.53 3.51	0.399 0.397	9.86 9.82 9.81	279.60 280.00
Experimental data.	[**9**]	3.90 4.71 4.97 5.00 5.02	1.87 1.89 1.93 1.95 2.03	9.200 14.869 17.67 18.122 18.363	3.137 3.434 3.461 3.505 3.691	0.34 0.39 0.41	---	---
	[**31**]	4.75	1.963	15.94	3.53	0.397	9.85	280.00
	[**32**]	4.74	1.96	15.91	3.51	0.40	9.82	280.00

The computationally generated elastic and thermodynamic properties of $Pd_{39}Ni_{10}Cu_{30}P_{21}$ BMG from the elastic part are given in **table 02.** The screening function S- influences more on the results of v_L and v_T than the rest in this group. The comparison of other such available theoretical [**29**, **30**] and experimental results [**9**, **31**, **32**] supports this computational work up to the most extent. The results generated by the BS-approach are higher than those obtained by the TG-approaches and best

matches with the experimental data. The presently proposed Shaw's model potential is found suitable to study the phonon dynamics of $Pd_{39}Ni_{10}Cu_{30}P_{21}$ and other such BMGs, where the influences of various local field correction functions are observed.

4. CONCLUSION:

Summing up this study, it may be concluded that the phonon dynamics of a BMG can be estimated by TG- and BS- approaches with the successful application of Shaw's model potential by supporting the present approach of PAA to provide important information of the BMG. The dielectric function is significant in the computation of the screening potential due to electron gas, and the local filed correction functions due to IU-, F- and S- are used in such observations. The relative effects of exchange and correlation in the selected properties are examined by these three different local field correction functions, which show substantial variations according to vibrational properties. The computed PDCs show extensive features of broad range collective excitations in $Pd_{39}Ni_{10}Cu_{30}P_{21}$ BMG and they are consistent with the other such and experimental data. The thermodynamic properties obtained due to BS-approach are higher than those due to TG-approaches. The calculated results of the BS approach are in excellent agreement with the experiment data compared to TG-approaches. The complete picture divulges the importance of local field correction function as well as the approaches in analysing the properties of the BMG.

References

I. M. Vora, Vibrational Dynamics of Binary Metallic Glasses, Lap Lambert Academic Publishing, Germany (2012).

II. A.M. Vora, Vibrational Dynamics of Bulk Metallic Glasses Studied by Pseudopotential Theory, Computational Materials, Ed. Wilhelm U. Oster, Nova Science Publishers, Inc., New York (2009), pp.119-176.

III. A. Inou, Mater. Trans., JIM, Vol. 37, (1996), p.1531.

IV. A. Inou, Mater. Trans., JIM, Vol. 37, (1996), p.1531.

V. A. Meyer, R. Busch and H. Schober, Phy. Rev. Lett., Vol. 83, (1999), p. 5027.

VI. L. M. Wang, Z. J. Zhan, J. Liu, L.L. Sun, G. Li and W. K. Wang, Journal of Physics: Condensed Matter, Vol. 13, (2001), pp. 5743–5748.

VII. V. M. Levin, J. S. Petronyuk, L. Wang and J. Hu, Mat. Res. Soc. Symp. Proc., Materials Research Society, (2003), p. 754.

VIII. L. M. Wang, G. Li, Z. J. Zhan, L.L. Sun and W. K. Wang, Philosophical Magazine Letters, Vol. 6-81, (2001), pp. 419 – 423.

IX. M. Jiang and L. Dai, Intrinsic correlation between fragility and bulk modulus in metallic glasses, (2007), Physical Review B, vol. 76, pp. 054204:1-7. DOI: 10.1103/PhysRevB.76.054204.

X. V. M. Levin et al., (2003), Mat. Res. Soc. Symp. Proc., pp. 1.18.1-6.

XI. J. Hubbard; J. L. Beeby, J. Phys. C: Solid State Phys, (1969), Vol. 2, pp. 556-571.

XII. S. Takeno; M. Goda, Prog. Thero. Phys., (1971), Vol. 45, pp. 331-352.

XIII. S. Takeno; M. Goda, Prog. Thero. Phys., (1972), Vol. 47, pp. 790-806.

XIV. A. B. Bhatia; R.N. Singh, Phys. Rev B., (1985), Vol. 31, pp. 4751-4758.

XV. M. M. Shukla; J. R. Campanha, Acta Phys. Pol. A., (1998), Vol. 94, pp. 655-660.

XVI. W. A. Harrison, Elementary Electronic Structure, (1999), World Scientific, Singapore.

XVII. R. Taylor, J. Phys. F: Met. Phys., (1978), Vol. 8, pp. 1699-1702.

XVIII. S. Ichimaru; K. Utsumi, Phys. Rev. B., (1981), Vol. 24, pp 7385-7388.

XIX. B. Farid; V. Heine; G. Engel, I. Robertson, J. Phys. Rev. B. (1993), Vol. 48, pp.11602-11621.

XX. A. Sarkar; D.S. Sen; S. Haldar; D. Roy, Mod. Phys. Lett., B. (1998), Vol. 12, pp. 639-648.

XXI. R. W. Shaw, Phy. Rev., (1968), Vol. 174, p. 769.

XXII. Gupta A.; Bhandari D.; Jain K. C.; Saxena N. S. Phys. Stat. Sol. (b). Vol. 95, (1996), pp. 367-374.

XXIII. W. A. Harrison, Pseudopotentials in the Theory of Metals, (1966), W. A. Benjamin, Inc.,

New York.
XXIV. J. M. Wills; W.A. Harrison, Phys. Rev B., (1983), Vol. 28, pp. 4363-4373.
XXV. E. T. Faber, Introduction to the Theory of Liquid Metals; (1972), Cambridge Uni. Press: London.
XXVI. V. Heine and D. Weaire, Solid State Physics 24, Eds. H. Ehrenreich, F. Seitz and D. Turnbull, Academic Press, New York (1970) p.249.
XXVII. L. I. Yastrebov and A. K. Katsnelson, Foundations of One-Electron Theory of Solids, (1987), Mir Publications, Moscow.
XXVIII. J. M. Ziman, Principal of the theory of the solids, 2nd edition, (1972), Cambridge Uni. Press, London.
XXIX. L. D. Sulir, M. Pyka and A. Kozlowski, Acta Phys. Pol. A. (1983), Vol. 63, pp. 435-443.
XXX. P. Chaudhari et al., Int. Conf. on Rec. Trends in App. Phy. & Mat. Sc., A.I.P. 1536, (2013), pp. 635-636. DOI:10.1063/1.4810387.
XXXI. W. H. Wang, The elastic properties, elastic models and elastic
XXXII. Perspectives of metallic glasses, Progress in Material Science, (2012), Vol. 57, pp. 487-656.
XXXIII. W. K. Wang, Materials transactions: Bulk metallic glasses-III, Vol. 42 (4), (2001), pp. 606-612.
XXXIV. W. H. Wang, F. Y. Li, M. X. Pan, D. Q. Zhao and R. J. Wang, Acta Materialia, (2004), Vol. 52, pp. 715-719.
XXXV. M. F. Thorpe, J. Non-Cryst. Sol. (1983), Vol. 57, pp.355-370.

****

Alkesh L. Gandhi
Department of Physics
C. U. Shah University
Gujarat

Aditya M. Vora
Department of Physics, Gujarat University
Ahmedabad